

Tissue measurement based on a multi-tap CMOS image sensor with binary structured light

Yuki Nishioka¹, Keiichiro Kagawa², Keita Yasutomi², and Shoji Kawahito²

¹ Graduate School of Engineering, Shizuoka University
3-5-1 Johoku, Hamamatsu, 432-8011 Japan

² Research Institute of Electronics, Shizuoka University
3-5-1 Johoku, Hamamatsu, 432-8011 Japan

E-mail: ynishiok@idl.rie.shizuoka.ac.jp

Abstract Preliminary experiments of deep tissue measurement with a highly-time-resolving CMOS image sensor and binary structured light are shown. Spatial and temporal responses of phantoms are studied.

Keywords: tissue imaging, spatial frequency domain imaging, time-resolved imaging, phasor

1. Introduction

Time-resolved imaging provides rich information in biomedical imaging, where laser pulses with a few to tens of pico-second duration excite tissues repeatedly and their temporal responses are measured. Lateral electric field charge modulator (LEFM)[1] has opened the pico-second regime ultra-high-speed computational imaging in a range of a few nano-seconds. The charge handling speed of LEFM is close to the limitation of charge transfer speed in silicon. In this paper, an application of LEFM-based image sensor to tissue imaging is explored.

2. Spatial and temporal frequency domain tissue imaging

Spatial frequency domain imaging (SFDI) provides two dimensional maps of absorption and reduced scattering coefficients, in which spatial frequency responses of the tissue are measured for at least two spatial frequencies[2]. In spite of its effectiveness, it is said that only the surface as deep as a few millimeters is observed with SFDI[3]. On the other hand, time domain measurement, which is often referred as time-resolved spectroscopy (TRS), provides deep tissue information depending on the source-detector separation. Our time-resolving CMOS image sensors have the potential to acquire huge information for various source detector separations at the same time with a binary structured pattern projection (Fig. 1).

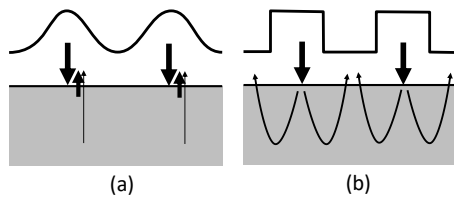


Fig. 1. (a) SFDI and (b) time-resolved imaging with a binary stripe pattern.

To analyze the temporal impulse response, a phasor method is useful. In this paper, a normalized and calibrated phasor method is utilized[4]. Assumed that an optical signal and an system function are given by $f(t)$ and $h(t)$, respectively, the measured signal, $g(t)$, is written as

$$g(t) = f(t) * h(t) \quad (1)$$

The frequency component is normalized and calibrated as follows

$$F_{NC}(v) = \left[\frac{G(v) / \sum g(t)}{H(v) / \sum h(t)} \right]^* \quad (2)$$

Note that x^* means the complex conjugate of a complex value, x . The measure in Eq. 2 is intensity-independent, and any data point is placed on or inside the circle with a radius of unity. Pulse width widening due to optical scattering is represented by rotation and amplitude reduction (Fig. 2). Tissue characteristics is well illustrated by a trajectory for multiple harmonics components.

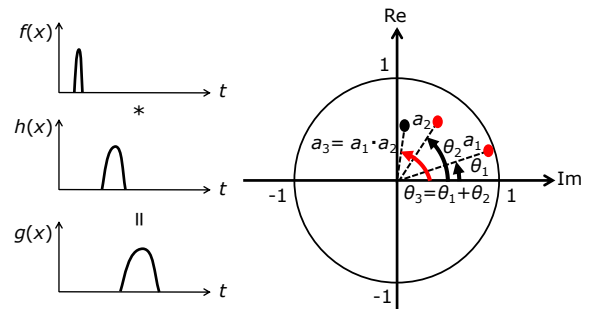


Fig. 2. Normalized and calibrated phasor plot.

3. Experimental results

Figure 3 shows an experimental setup. A time-resolving CMOS image sensor designed for fluorescence lifetime imaging was utilized[5]. As an impulse light source, super continuum laser (NKT, SuperK Extreme EXB-6, 19.49MHz with a pulse picker) was used and a wavelength of 650nm by a bandpass filter of 650nm \times 25nm was inserted. 33 images were captured with a unit delay of 106.9ps and inter-frame subtraction was performed to reproduce transient images. Figure 4 shows a cross-section of a 2-layer silicone phantom, which is approximately 100mm \times 100mm \times 20mm in size. A bulk phantom made by material-1 was made for comparison. To emulate a material-2 bulk, light was incident from the bottom of the 2-layer phantom because it was thick enough.

Table 1 shows measured optical properties of the silicone phantoms at a wavelength of 850nm. Note that the absorption coefficients of the 2-layer phantom is between those of material-1 and -2, but more likely to the surface layer (material-1). The reduced scattering coefficients were as much as that of material-1 (surface layer), which means only the surface layer was observed with SFDI.

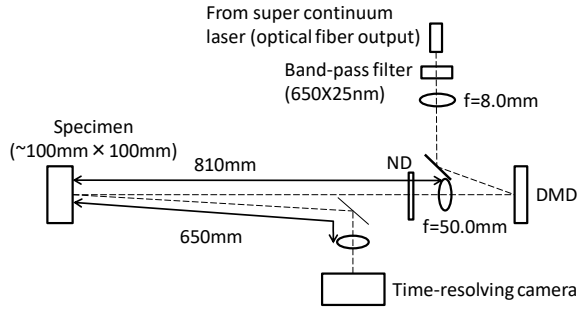


Fig. 3. Experimental setup.

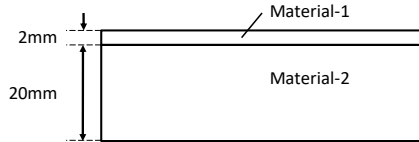


Fig. 4. Cross-section of a 2-layer phantom.

Table 1. Measured optical properties by SFDI for spatial frequencies of (a) 0.1/mm and (b) 0.2/mm.

(a)		
	μ_a [mm^{-1}]	μ'_s [mm^{-1}]
Material-1 (bulk)	0.0255	0.8270
Material-2 (bulk)	0.0139	0.6373
2-layer phantom	0.0228	0.8270

(b)		
	μ_a [mm^{-1}]	μ'_s [mm^{-1}]
Material-1 (bulk)	0.0252	0.8185
Material-2 (bulk)	0.0140	0.6402
2-layer phantom	0.0223	0.8128

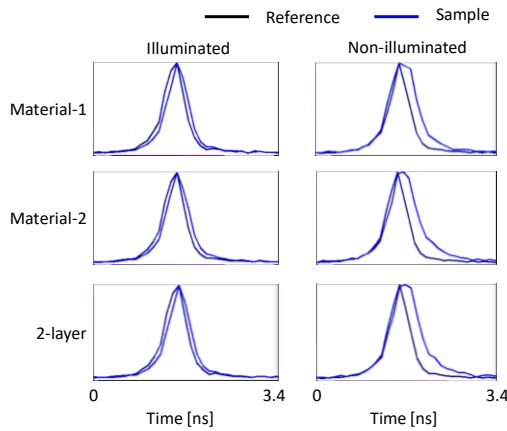


Fig. 5. Measured temporal waveforms.

Figures 5-7 show the results of time-resolved imaging for a binary stripe pattern projection with a spatial period of 20mm (=spatial frequency of 0.05/mm). Although a significant difference is not observed in the temporal responses of the phantoms as shown in Fig. 5, the phase map of the 2-layer phantom is more similar to that of the deep layer (material-2) in the middle of the non-illuminated regions (Fig. 6). Note that the phase of the illuminated regions became only noise because their pixel values were saturated to obtain moderate signal intensity in the non-illuminated regions.

Figure 7 shows a very interesting behavior. The trajectory of the 2-layer phantom in the illuminated region is between those of material-1 and -2. However, that of the 2-layer phantom in the non-illuminated region is very similar to that of material-2. In this situation, the maximal source-detector separation was 5mm, so that light that traveled in slightly deep region was detected in the middle of the non-illuminated region.

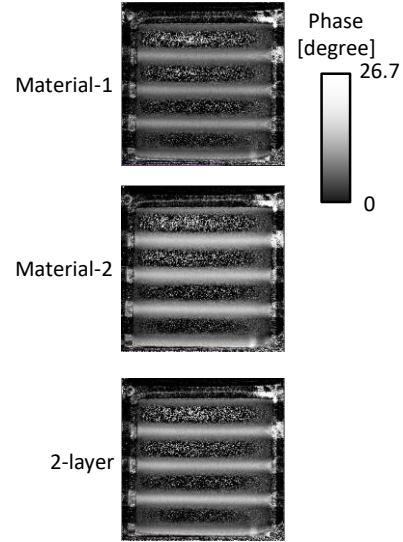


Fig. 6. Measured phase maps.

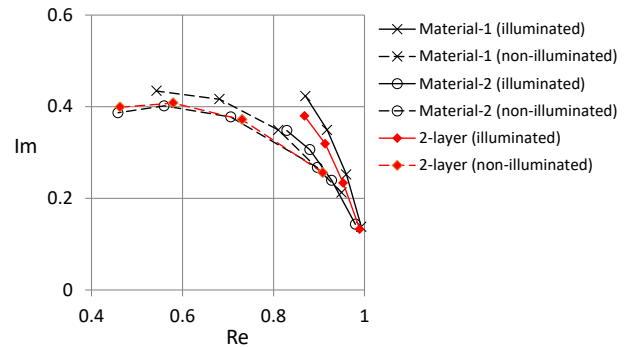


Fig. 7. Measured trajectories for 1st to 4th harmonics.

4. Conclusion

LEFM-based time-resolving CMOS image sensor was applied to 2-layer tissue phantom imaging. With a combination of binary stripe pattern projection, the potential of deeper tissue measurement was suggested.

Acknowledgements

This work was partially supported by Grant-in-Aid for Scientific Research (B) Number 18H05240, and (S) Numbers 17H016012 and 18H05240.

References

- [1] S. Kawahito, G. Baek, Z. Li, S. Han, M. Seo, K. Yasutomi and K. Kagawa, "CMOS lock-in pixel image sensors with lateral electric field control for time-resolved imaging," *International Image Sensor Workshop*, 10.06, pp. 1417-1429 (2013).
- [2] D. Cuccia, F. Vevillacqua, A. Durkin, F. Ayers, and B. Tromberg, "Quantitation and mapping of tissue optical properties using modulated imaging," *J. Biomed. Opt.*, Vol. 14, 02412 (2009).
- [3] T. O'Sullivan, A. Cerussi, D. Cuccia, and B. Tromberg, "Diffuse optical imaging using spatially and temporally modulated light," *J. Biomed. Opt.*, Vol. 17, 071311 (2012).
- [4] R. Miyagi, K. Kagawa, Y. Murakami, H. Nagahara, K. Yasutomi, and S. Kawahito, "Visualization of time-of-flight signals with normalized and calibrated phasor plot," in *Proc. Int'l Workshop on Image Sensors and Imaging Systems (IWISS2018)* (2018, to appear).
- [5] M. -W. Seo, K. Kagawa, K. Yasutomi, T. Takasawa, Y. Kawata, N. Teranishi, Z. Li, I. A. Halin, S. Kawahito, "A 10.8ps-time-resolution 256x512 image sensor with 2-tap true-CDS lock-in pixels for fluorescence lifetime imaging," *ISSCC Dig. Tech. Papers*, pp. 189-199 (2015).